Alfaro-Aco et al., https://doi.org/10.1083/jcb.201607060

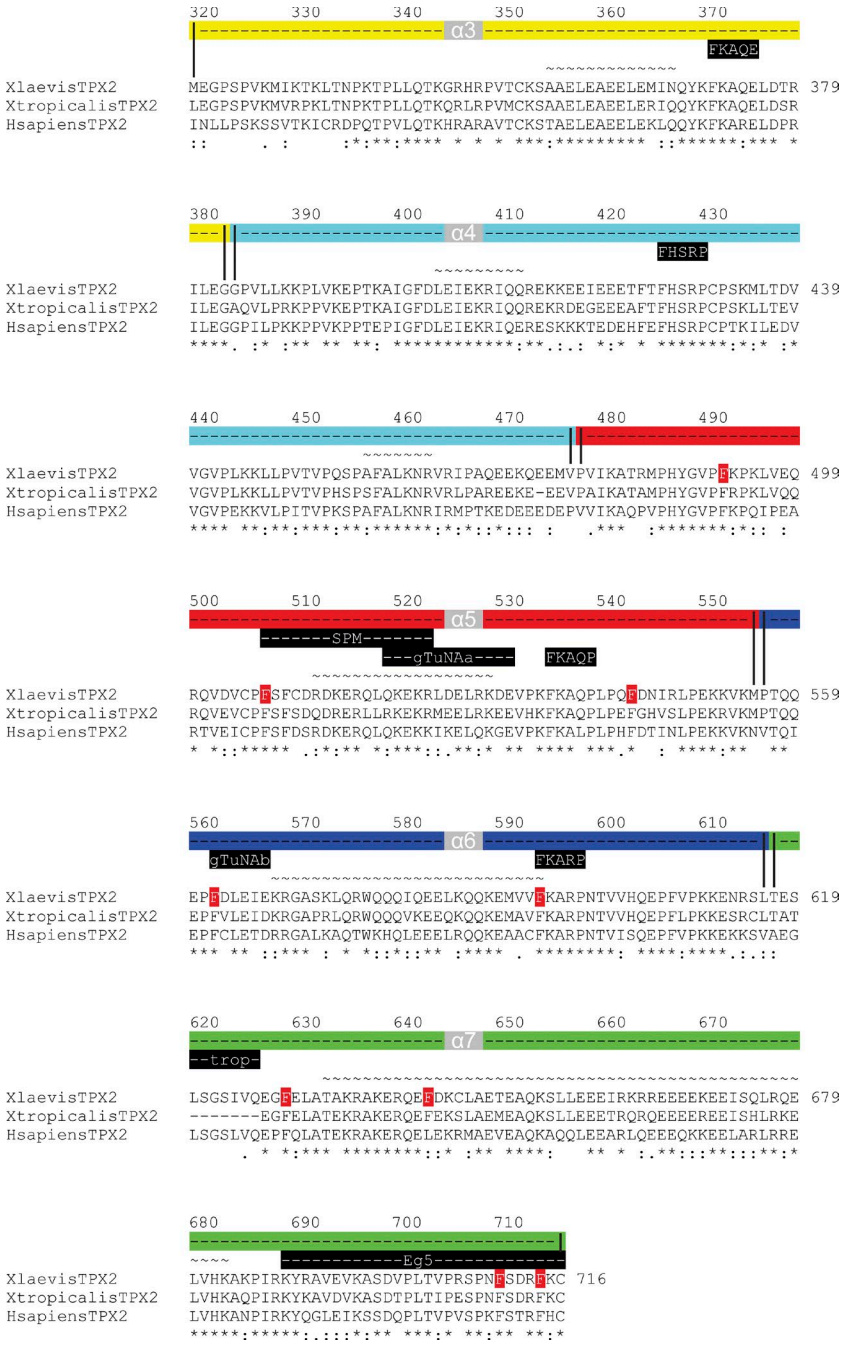

Figure S1. **Secondary structure of TPX2.** The *X. laevis* TPX2 sequence was aligned with dozens of other TPX2 sequences before being subjected to secondary structure analysis using the program Jpred. Only three sequences are shown in the alignment for simplicity. Amino acid residues are numbered in regular intervals. A-Helical regions are depicted as ~. Defined domains are highlighted in different colors and separated by vertical lines. Important motifs are indicated in black with white script, and single-site mutations are colored red with white script.

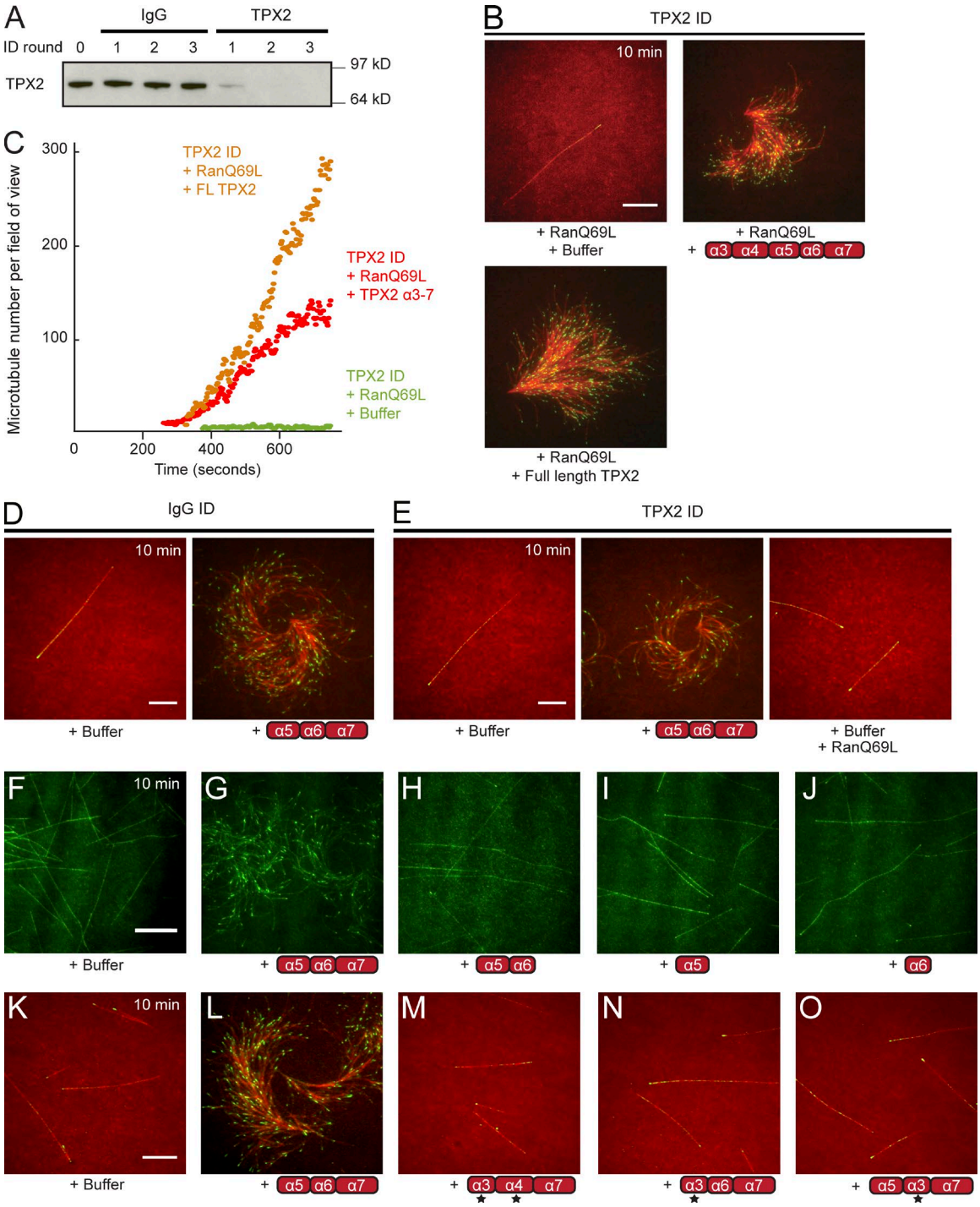

Figure S2. **The N-terminal half of TPX2 contributes to achieve higher levels of branching MT nucleation, but TPX2 α5–α7 is the minimal construct that can substitute endogenous TPX2.** (A) Immunodepletion (ID) of TPX2 from *Xenopus* egg extract. (B) Branching MT nucleation in TPX2-depleted extracts supplemented with 10 µM RanQ69L, testing the activity of 1 µM TPX2 α3–α7 and1 µM full-length TPX2. A reaction with 10 µM RanQ69L only was used to confirm the loss of endogenous TPX2 activity. EB1-GFP (green) and Cy5-labeled porcine brain tubulin (red) were added to the extract to follow MT plus ends and MTs, respectively. (C) The number of individual MTs was counted for each time frame and then plotted against time. The data are displayed for addition of TPX2 constructs in B. (D) Branching MT nucleation in control IgG-depleted *Xenopus* egg extracts and in the presence or absence of 1 µM TPX2 α5–α7. The assay was performed as in B. All images were taken after 10 min. Brightness and contrast were adjusted for each image individually to optimize visual comparison of MT structures. (E) Same as D, except endogenous TPX2 was removed via immunodepletion. A reaction with 10 µM RanQ69L was used to confirm the loss of endogenous TPX2 activity. (F–J) Branching MT nucleation in *Xenopus* egg extracts with 1 µM truncated TPX2 constructs. Alexa Fluor 488–labeled porcine brain tubulin (green) and EB1-GFP (green) were added to visualize MTs, and vanadate was added to prevent dynein-mediated MT gliding. All images were acquired after 10 min. Brightness and contrast were adjusted for each image individually to optimize visual comparison of MT structures. (K–O) Branching MT nucleation in *Xenopus* egg extracts in the presence of 1 µM TPX2 α5–α7 with domains α5 and α6 substituted. The assay was performed as in F–J, except EB1-GFP (green) and Alexa Fluor 568–labeled porcine brain tubulin (red) were added to follow the MT plus ends and to visualize MTs, respectively. Tests in F–O were performed in the presence of endogenous TPX2. All extract experiments were performed at least three different times. Bars, 10 µm.

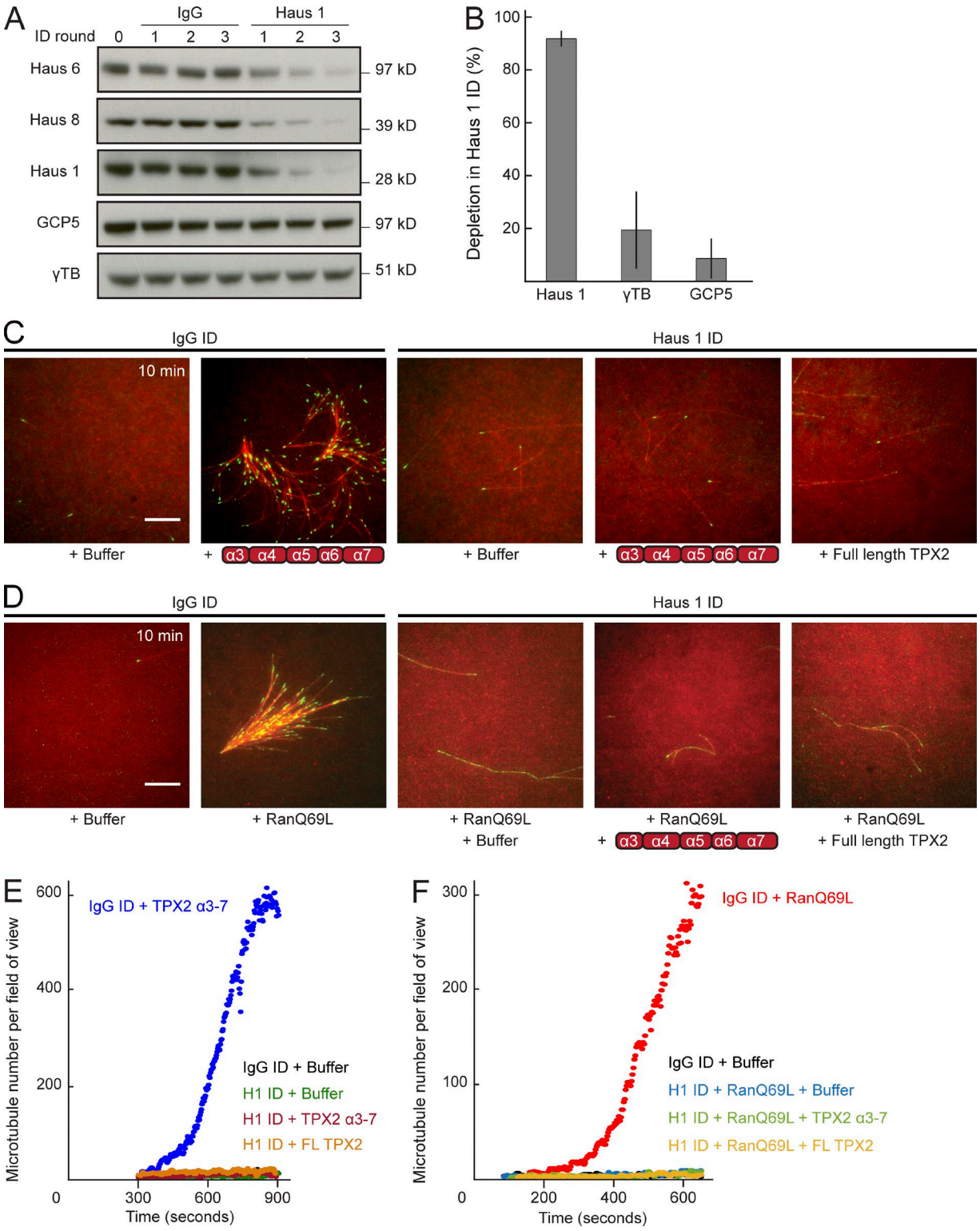

Figure S3. **TPX2 requires the augmin complex to induce MT nucleation.** (A) Immunodepletion (ID) of the augmin complex via an antibody against the augmin subunit Haus 1 from *Xenopus* egg extract. (B) Quantification of Haus 1, γ-tubulin, and GCP5 depletion in Haus 1–immunodepleted extracts. Means were calculated from three different immunodepletions. Error bars represent standard deviation. (C) Branching MT nucleation in control IgG-depleted *Xenopus* egg extract and in the presence or absence of 1 µM TPX2 α3–α7. Augmin-depleted *Xenopus* egg extract was used to test 1 µM full-length TPX2 and 1 µM TPX2 α3–α7. EB1-GFP (green) and Cy5-labeled porcine brain tubulin (red) were added to the extract to follow MT plus ends and MTs, respectively. Vanadate was added to prevent dynein-mediated MT gliding. All images were taken after 10 min. Brightness and contrast were adjusted for each image individually to optimize visual comparison of MT structures. (D) Same as C, except control IgG-depleted *Xenopus* egg extract was tested in the presence or absence of 10 µM RanQ69L. The reactions in augmin-depleted *Xenopus* egg extract were all done in the presence of 10 µM RanQ69L. Bars, 10 µm. (E) The number of individual MTs was counted for each time frame and then plotted against time. The data are displayed for addition of TPX2 constructs in C. (F) Same as E, except the data are displayed for addition of TPX2 constructs in D. All extract experiments were repeated at least three different times.

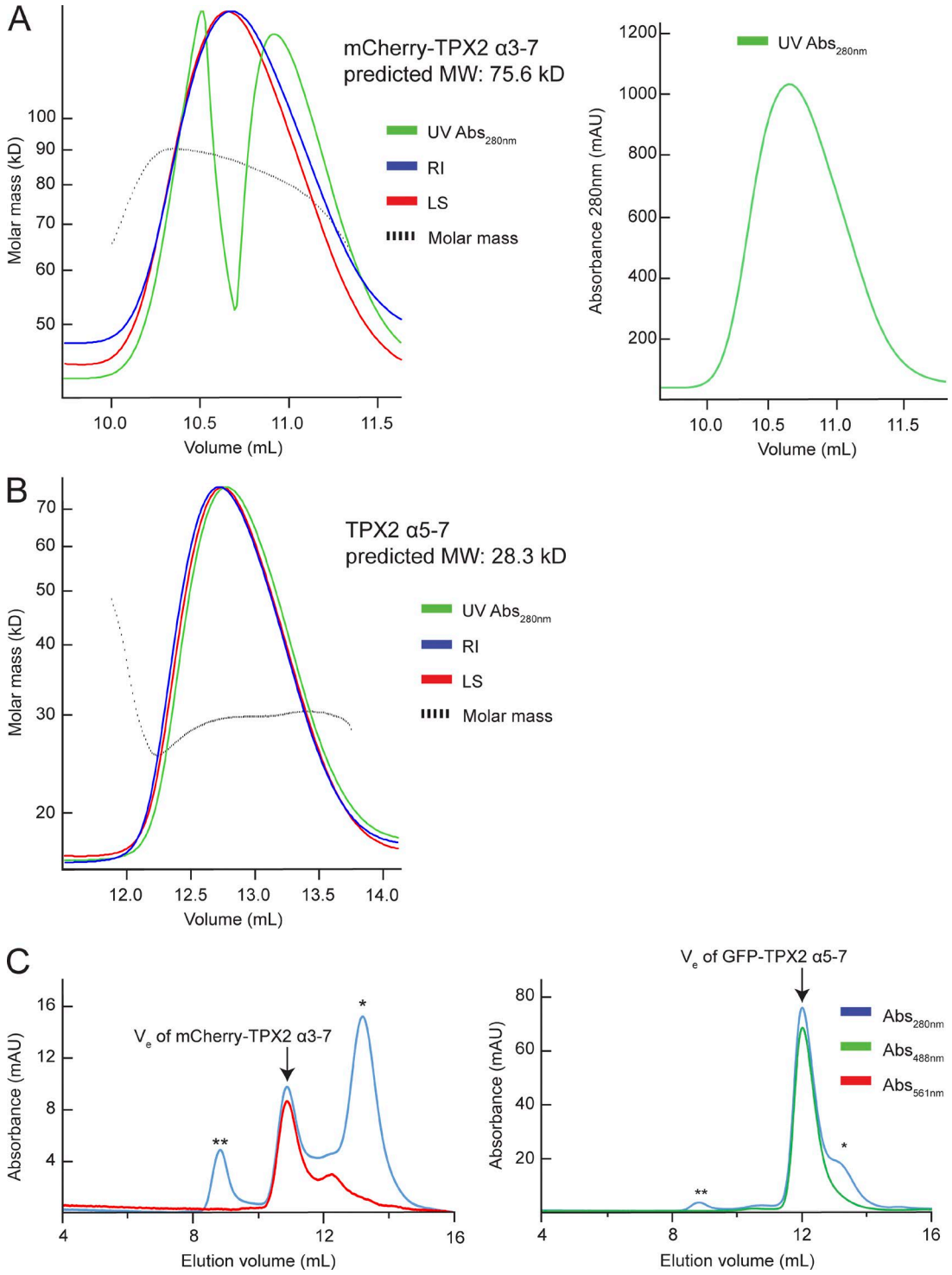

Figure S4. **TPX2 constructs are monomeric and do not bind tubulin dimers.** (A) SEC-MALS analysis of N-His6-mCherry TPX2 α3–α7 reveals the protein is monomeric in solution. Although the UV absorbance trace of the MALS instrument (left) is interrupted, the original UV absorbance trace from the SEC run (right) is indeed accurate and still allows the refractive index (RI) and light scattering (LS) peaks to overlap, albeit not perfectly. This does not change the result of the analysis. (B) Same as A but testing untagged TPX2 α5–α7, which also appears to be monomeric in solution. (C) Chromatogram of 5 µM N-His6-mCherry TPX2 α3–α7 (left) and 5 µM N-His6-GFP TPX2 α5–α7 (right) incubated with 0.35 mg/ml unpolymerized tubulin and subjected to gel filtration. Arrows mark the elution volume of the TPX2 construct alone (determined from an independent run). The elution volume of dimeric tubulin is marked by one asterisk (*), and tubulin aggregates in the void volume are marked by two asterisks (**; determined from an independent run). The peaks of TPX2 α3–α7 and TPX2 α5–α7 are not shifted upon their incubation with tubulin, indicating that neither construct appears to interact with tubulin. These assays were performed once.

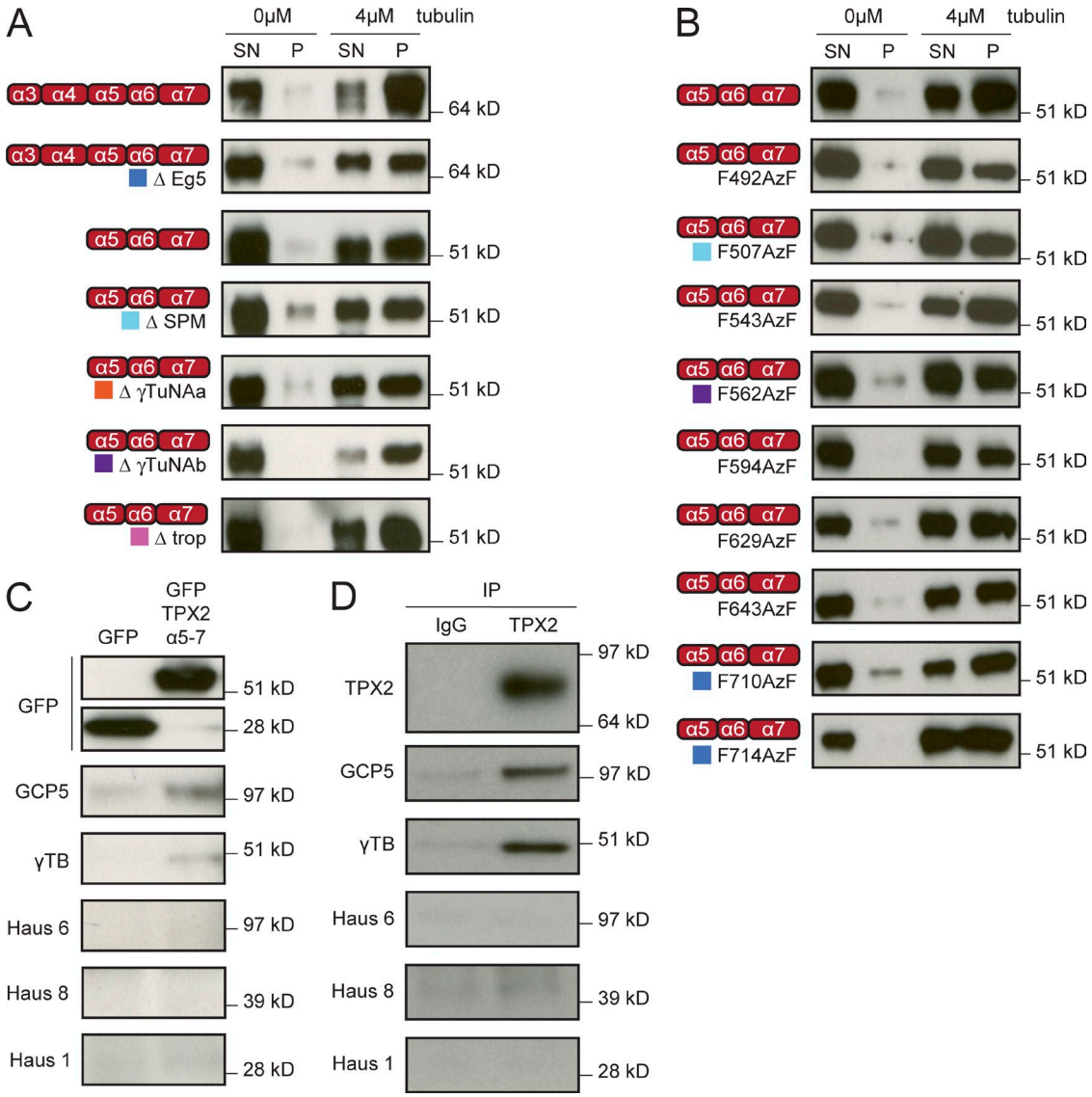

Figure S5. **All versions of the minimal TPX2 α5–α7 bind MTs, but TPX2 α5–α7 does not interact strongly with the augmin complex.** (A) Co-sedimentation assay of 0.5 μM of the different TPX2 deletion constructs with Taxol-stabilized MTs in vitro. Each protein was detected via immunoblotting using an antibody against TPX2. (B) Same as A except with TPX2 α5–α7 containing different single-site mutations. Each protein was detected via immunoblotting using an antibody against GFP. (C) Immunoprecipitation of 1 μM GFP-tagged TPX2 α5–α7 from *Xenopus* egg extract using an antibody specific against GFP. The same GFP antibody was used for detection in the immunoblot, along with antibodies against Haus 6, Haus 8, Haus 1, GCP5, and γ-tubulin. (D) Immunoprecipitation of endogenous TPX2 from *Xenopus* egg extract in the presence of 10 μM RanQ69L using an antibody against TPX2. RanQ69L was added to release TPX2 from importin α/β inhibition. The same TPX2 antibody was used for detection in the immunoblot, along with antibodies against Haus 6, Haus 8, Haus 1, GCP5, and γ-tubulin. Experiments in A and B were repeated three times, and experiments in C and D were repeated two times. SN, supernatant; P, pellet; IP, immunoprecipitation.

Table S1. **TPX2 expression constructs used in this study**

Construct name	Tag	TPX2 amino acids
α3–α7	N-GST-thrombin	320–716
α3–α6	N-GST-thrombin	320–616
α3–α5	N-GST-thrombin	320–555
α3–α4	N-GST-thrombin	320–477
α3	N-GST-thrombin	320–384
α7	N-GST-thrombin	616–716
α6–α7	N-GST-thrombin	558–716
α5–α7	N-GST-thrombin	478–716
α4–α7	N-GST-thrombin	385–716
α3	N-His6-GFP-TEV	321–385
α3–α4	N-His6-GFP-TEV	321–476
α5–α6	N-His6-mCherry-TEV	477–616
α7	N-His6-GFP-TEV	617–716
Full length	N-Strep-His6-TEV-mCherry	1–716
α5	N-GST-thrombin	478–555
α6	N-GST-thrombin	556–616
α5–α6	N-GST-thrombin	478–616
α3–α4–α7[a]	N-GST-thrombin	320–429 + 617–716
α5–α3–α7[a]	N-GST-thrombin	430–555 + 320–383 + 617–716
α3–α6–α7[a]	N-GST-thrombin	320–383 + 556–716
α3–α7 ΔEg5	N-GST-thrombin	320–688
α5–α7 ΔSPM	N-GST-thrombin	478–506 + 524–716
α5–α7 ΔγTuNAa	N-GST-thrombin	478–517 + 532–716
α5–α7 ΔγTuNAb	N-GST-thrombin	478–560 + 571–716
α5–α7 Δtrop	N-GST-thrombin	478–619 + 627–716
α3–α7	N-His6-mCherry-TEV	321–716
α5–α7	N-His6-GFP-TEV	477–716
α5–α7	N-GFP-TEV + C-His6	477–716
α5–α7 F492AzF	N-GFP-TEV + C-His6	477–716 F492AzF
α5–α7 F507AzF	N-GFP-TEV + C-His6	477–716 F507AzF
α5–α7 F543AzF	N-GFP-TEV + C-His6	477–716 F543AzF
α5–α7 F562AzF	N-GFP-TEV + C-His6	477–716 F562AzF
α5–α7 F594AzF	N-GFP-TEV + C-His6	477–716 F594AzF
α5–α7 F629AzF	N-GFP-TEV + C-His6	477–716 F629AzF
α5–α7 F643AzF	N-GFP-TEV + C-His6	477–716 F643AzF
α5–α7 F710AzF	N-GFP-TEV + C-His6	477–716 F710AzF
α5–α7 F714AzF	N-GFP-TEV + C-His6	477–716 F714AzF

For each TPX2 construct generated and used in this study, the name, tag, and exact amino acids covered are indicated.
[a]Separate sequences were linked by Gly-Ser-Gly.

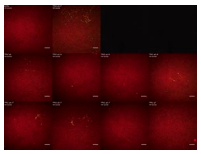

Video 1. **Branching MT nucleation activity of truncated TPX2 constructs (related to Fig. 1).** Branching MT nucleation in *Xenopus* egg extracts in the presence of 2 µM of different truncated TPX2 constructs. The same results were obtained with a lower TPX2 concentration of 0.75 µM. EB1-GFP (green) and Alexa Fluor 568–labeled porcine brain tubulin (red) were added to follow MT plus ends and MTs, respectively. Vanadate was added to prevent dynein-mediated MT gliding. Elapsed time is shown in seconds and time-point zero marks when the reaction was started. Individual frames were collected every 2 s, and the video is played at 15 frames per second. Brightness and contrast were adjusted for each movie individually to optimize visual comparison of MT structures. Bar, 10 µm.

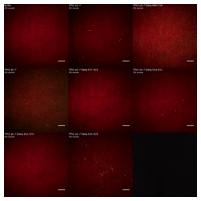

Video 2. **Branching MT nucleation activity of TPX2 with motif deletions (related to Fig. 4).** Branching MT nucleation in *Xenopus* egg extracts in the presence of different deletion mutants of TPX2 α3–α7 and α5–α7 (2 µM). The same results were obtained with a lower TPX2 concentration (0.75 µM). EB1-GFP (green) and Alexa Fluor 568–labeled porcine brain tubulin (red) were added to follow the MT plus ends and MTs, respectively. Vanadate was added to prevent dynein-mediated MT gliding. Elapsed time is shown in seconds and time-point zero marks when the reaction was started. Individual frames were collected every 2 s, and the movie is played at 15 frames per second. Brightness and contrast were adjusted for each movie individually to optimize visual comparison of MT structures. Bar, 10 µm.

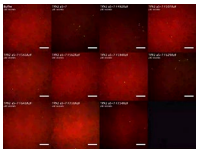

Video 3. **Branching MT nucleation activity of TPX2 α5–α7 with single-site mutations (related to Fig. 5).** Branching MT nucleation in *Xenopus* egg extracts in the presence of TPX2 α5–α7 with single-site mutations (2 µM). The same results were obtained with a lower TPX2 concentration of 1 µM. Movies for F492AzF, F629AzF, and F714AzF mutants, which show a high level of activity, as well as the movie for the positive control TPX2 α5–α7, were collected using one extract. Movies for the rest of the mutants and the negative control were collected with a different extract. This was necessary because the lifetime of one extract was incompatible with the high number of samples, however, both controls are representative and consistent among all extracts tested. EB1-mCherry (green) and Cy5-labeled porcine brain tubulin (red) were added to the extract to follow MT plus ends and MTs, respectively. Vanadate was added to prevent dynein-mediated MT gliding. Elapsed time is shown in seconds and time-point zero marks when the reaction was started. Individual frames were collected every 8 s, and the movie is played at five frames per second. Brightness and contrast were adjusted for each movie individually to optimize visual comparison of MT structures. Bar, 10 µm.